

Pomeron dominance in deeply virtual Compton scattering and the femto holographic image of the proton

D. Müller

Department of Physics and Astronomy, Arizona State University, Tempe, AZ 85287-1504, USA

The dominance of the soft pomeron in soft high energy scattering and the evolution to the deeply virtual regime, predicted by perturbation theory, allow us to reveal generalized parton distributions from H1 and ZEUS measurements of deeply virtual Compton scattering. These distributions encode a holographic image of the proton, which will be presented.

We study deeply virtual Compton scattering (DVCS) off the proton at high energies and aim to reveal generalized parton distributions (GPDs) [1] from HERA measurements [2]. The GPDs then yield a 3D image of quark and gluon distributions at small longitudinal momentum fraction x . The analysis substantially relies on the soft pomeron dominance in the non-perturbative sector. Various points of view on the pomeron are recalled before the DVCS predictions are derived in a simple, however, approximated analytic form and the analysis is performed.

In soft high energy scattering experiments, i.e., no further large scale is present, the energy dependence of scattering amplitudes is described within Regge phenomenology as an exchange of particles in the t (momentum transfer squared) channel, see Fig. 1(a). Theoretical considerations, based on partial wave decomposition, analyticity, and crossing, predict that scattering amplitudes behave at large center-of-mass energy squared s as $s^{\alpha(t)}$, where $\alpha(t) = \alpha(0) + \alpha't$ is the leading Regge trajectory in terms of the intercept $\alpha(0)$ and slope α' . Such a trajectory relates the particle spin $J = \alpha(m^2)$ with its mass. To explain experimental measurements, the trajectory $\alpha_{\mathbb{P}}(t) = 1.08 + 0.25t$ has been introduced [3]. It is associated with a hypothetical spin-one quasi particle, the so-called soft pomeron that carries the vacuum quantum numbers. No particles belonging to this pomeron trajectory could be established and so it remains exceptional.

The notion pomeron is also applied in the phenomenology of (semi) hard reactions. The HERA measurements, where a 27 GeV electron/positron beam collides with a 820 GeV proton one, lead to the discovery that the energy dependence of cross sections get steeper with growing photon virtuality $Q^2 = -q_1^2$. Let us consider the proton structure function $F_2(x_{\text{Bj}}, Q^2)$, measured in deep inelastic scattering (DIS), at small x_{Bj} . The reciprocal Bjorken scaling variable $1/x_{\text{Bj}} = 2P_1 \cdot q_1/Q^2$, where P_1 is the proton momentum, is nearly proportional to the photon-proton center-of-mass energy squared $W^2 = (q_1 + P_1)^2$. F_2 possesses an almost flat $1/x_{\text{Bj}}$ dependence at low $Q^2 < Q_0^2 \sim 1\text{GeV}^2$ and gets steeper with increasing Q^2 :

$$F_2(x_{\text{Bj}}, Q^2) \sim (1/x_{\text{Bj}})^{\lambda(Q^2)}, \quad (1)$$

where $\lambda(Q^2) \gtrsim 0$ rises with growing Q^2 .

In Regge theory $\lambda = \alpha_{\mathbb{P}}(0) - 1$ is considered as Q^2 independent, which is incongruous with experiment. To cure

this issue, a double pomeron exchange within a soft and hard pomeron, e.g., $\alpha_{\mathbb{P}}^{\text{hard}}(0) \approx 1.4$, was suggested [4]. The (energy ordered) resummation of the gluon ladder in the BFKL approach results the perturbative pomeron, which indeed possesses such a large intercept [5]. However, the theoretical understanding remains poor.

Fortunately, perturbative QCD predicts the variation of observables with respect to a hard scale. F_2 is the absorptive part of the forward Compton amplitude. Analogous to Fig. 1(b), it factorizes in terms of quark $q(x, Q^2)$ and gluon $G(x, Q^2)$ densities. Their scale changes are governed by evolution equations, written for the Mellin-moments, e.g., $G_n(Q^2) = \int_0^1 dx x^{n-1} G(x, Q^2)$, as

$$Q^2 \frac{d}{dQ^2} \begin{pmatrix} \Sigma_n \\ G_n \end{pmatrix} = \begin{pmatrix} \Sigma\Sigma\gamma_n & \Sigma G\gamma_n \\ G\Sigma\gamma_n & GG\gamma_n \end{pmatrix} \begin{pmatrix} \Sigma_n \\ G_n \end{pmatrix}. \quad (2)$$

Here $\Sigma_n = \sum_q q_n$ is the flavor singlet quark density and $^{AB}\gamma_n$ are the anomalous dimensions, depending on spin n . The gluon-gluon and gluon-quark anomalous dimensions possess a ‘pomeron’ pole at spin $n = 1$. Solving the evolution equation yield an exponentiation of this pole. In x -space this converts to the so-called double log approximation, see below. This resummation of large contributions might be effectively parameterized as in (1).

The DIS measurements are well described by perturbative QCD, where the input parton densities are extracted from global fits. It has been suggested to generate dynamically sea quarks and gluon densities by evolution [6]. Starting from a very low input scale, fine tuning is required to fit experimental data. In the small x region the evolution is mainly driven by the ‘pomeron’ pole of the anomalous dimensions and data are indeed consistent with the double log approximation [7]. Both approaches were combined within a soft pomeron like input [8], where only the initial scale, two normalization factors,

$$\Sigma_n(Q_0) = \frac{N_{\Sigma}}{n - \alpha_{\mathbb{P}}(0)}, \quad G_n(Q_0) = \frac{N_G}{n - \alpha_{\mathbb{P}}(0)}, \quad (3)$$

and perhaps the running coupling have to be adjusted.

The dynamical generation of parton densities for small x_{Bj} is perhaps the most predictive approach to DIS. Although the ‘pomeron’ pole in the evolution operator is essential, the resulting parton densities depend on the non-perturbative input, too. Since real Compton scattering

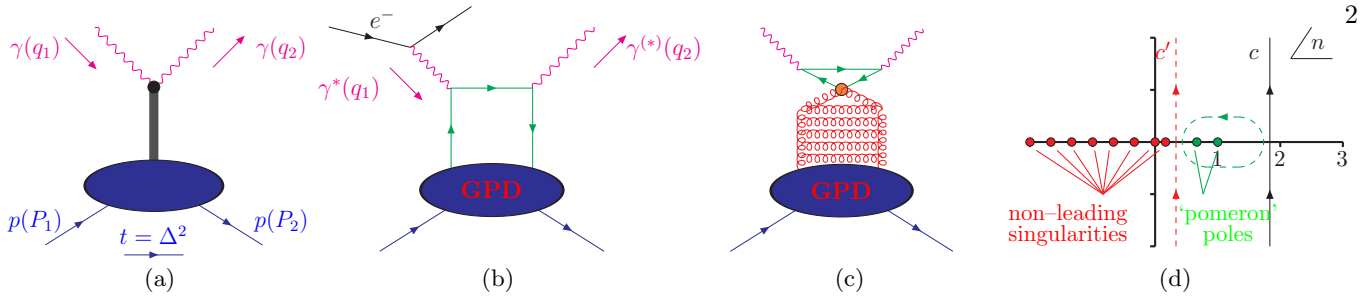


FIG. 1: The Compton scattering amplitude (a) at high energy and small t is dominated by the pomeron exchange in the t -channel. The lowest order perturbative contribution to DVCS at the scale $Q^2 = -q_1^2$ and at a very low input scale is shown in (b) and (c), respectively. The integration path used in Eq. (4) and its deformation in the complex n -plane are shown in (d).

can be described at high energy within soft pomeron exchange [9], it is apparent that the non-perturbative input is dominated at a low scale by the soft pomeron, too. It arises in the expectation value of operators, sandwiched between proton states, as pole contribution (3).

Let us apply this conjecture to DVCS. At leading order (LO) the factorization of the amplitude is given by the hand-bag diagram, depicted in Fig. 1(b), in terms of Compton form factors (CFFs) [10]. At small $\xi \cong x_{Bj}/2$ only the flavor singlet part of the helicity conserved and charge even CFF $\mathcal{H}(\xi, t, Q^2 = -q_1^2)$ is relevant [11]. To diagonalize the evolution operator, the complex conformal partial wave decomposition will be employed [12, 13]

$$\mathcal{H}^S = \frac{1}{2i} \int_{c-i\infty}^{c+i\infty} dn \frac{\Gamma(n+3/2)}{\Gamma(3/2)\Gamma(2+n)} \left[i - \cot\left(\frac{\pi n}{2}\right) \right] (4) \\ \times \left(\frac{2}{\xi}\right)^n (Q_S^2, 0) \mathbb{E}_n(Q^2, Q_0^2) \begin{pmatrix} \Sigma_n \\ G_n \end{pmatrix} (\xi, t, Q_0^2).$$

Here the singularities in the complex n -plane are on the l.h.s. of the integration path, cf. Fig. 1(d). $Q_S^2 = \sum_q Q_q^2/n_f$ is the averaged charge square fraction for n_f active quarks. Σ_n and G_n are conformal GPD moments, which reduce in the forward case to the parton density ones. The evolution operator \mathbb{E}_n , a 2×2 matrix, is the same as in DIS, see, e.g., Ref. [8]. By means of \mathbb{P}_n^\pm projectors it might be decomposed in ‘+’ and ‘-’ eigenmodes:

$$\mathbb{E}_n(Q^2, Q_0^2) = \mathbb{P}_n^+ \left(\frac{\alpha_s(Q)}{\alpha_s(Q_0)} \right)^{\lambda_n^+} + \mathbb{P}_n^- \left(\frac{\alpha_s(Q)}{\alpha_s(Q_0)} \right)^{\lambda_n^-}, (5)$$

where λ_n^\pm are eigenvalues of the anomalous dimension matrix, appearing in Eq. (2). The running coupling

$$\alpha_s(Q) = \frac{4\pi}{(11 - 2n_f/3) \ln(Q^2/\Lambda_{\text{QCD}}^2)} (6)$$

is parameterized by Λ_{QCD} .

To illuminate the physics at small x_{Bj} , let us derive the double log approximation for \mathcal{H}^S (4). The dominant contribution comes from the most right-lying singularity, see Fig. 1(d). If $\alpha_{\mathbb{P}}(t) < 1$, this is an essential singularity appearing in the ‘+’-mode of the evolution operator (5),

$$\lambda_n^+ = -\frac{\lambda}{n-1} + \bar{\lambda}^+ + O(n-1), \quad \lambda = \frac{36}{33 - 2n_f}. (7)$$

For $0 < \alpha_{\mathbb{P}}(t)$ the next-leading singularity is expected to be the soft pomeron pole. To simplify the analysis, we set $\alpha_{\mathbb{P}}(0) = 1$. Hence, for $t = 0$ this singularity joins the leading one and both of them should be considered in Eq. (4). They can be encircled by a deformation of the integration contour, as shown in Fig. 1(d). The remaining background integral (dashed integration path c') can be safely neglected. Next the variable transformation $n = 1 + \rho j$ with $\rho = [\lambda \ln(\alpha_s(Q_0)/\alpha_s(Q))/\ln(2/\xi)]^{1/2}$ and $Q > Q_0$ is performed, where ρ is considered as small. Taylor expansion at $\rho = 0$ yield integrals that reduce for $t = 0$ to the modified Bessel function $I_a(\sigma)$ with $a = 0, 1, \dots$:

$$I_a(\sigma, \bar{\alpha}t) = \frac{1}{2i\pi} \oint_{(0, \bar{\alpha}t)} dj \frac{j^a}{j - \bar{\alpha}t} e^{\sigma(j+1/j)/2}, (8)$$

where $\sigma^2 = 4\lambda \ln[\alpha_s(Q_0)/\alpha_s(Q)] \ln[2/\xi]$. The effective slope $\bar{\alpha} = \alpha_{\mathbb{P}}'/\rho$ depends on ξ and Q . Note that the asymptotic behavior of the integral (8) is a independent:

$$I_a(\sigma, \bar{\alpha}t) = \frac{1}{1 - \bar{\alpha}t} \frac{e^\sigma}{\sqrt{2\pi\sigma}} \quad \text{for } \sigma \rightarrow \infty.$$

Now the GPD moments have to be specified. In the presence of a hard scale the partonic content of the pomeron can be resolved [14]. It is expected that the pomeron is mainly made of glue, see e.g., Ref. [15]. For simplicity the quark distribution, including the valence quarks, will be neglected in the small x region. Finally, the CFF (4) reads in the double log approximation as

$$\mathcal{H}^{\text{DL}} = \frac{i\pi n_f Q_S^2}{6\xi} \left[\rho I_1(\sigma, \bar{\alpha}t) \left(\frac{\alpha_s(Q)}{\alpha_s(Q_0)} \right)^{\bar{\lambda}^+} G_1(\xi, t, Q_0^2) \right. \\ \left. + \text{pole term} \right] + O(\rho^2), (9)$$

where $\bar{\lambda}^+ = 1 + 20n_f/9(33 - 2n_f)$. Here the pole term comes from the soft pomeron in the ‘-’ mode. It is an unsubstantial contribution that vanishes for $t = 0$. The real part of \mathcal{H}^S is induced by subleading terms in ρ and will not be considered here. We remark that the optical theorem $F_1 = \Im\mathcal{H}/(2\pi)|_{q_2 \rightarrow q_1}$ and the Callan-Gross

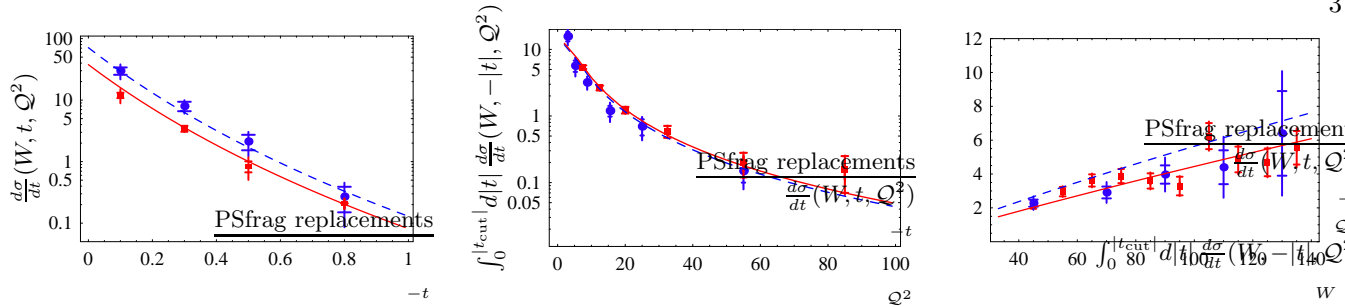


FIG. 2: In the left panel the t -dependence of the differential DVCS cross section (12) is fitted to H1 data for $W = 71$ GeV, $Q^2 = 4$ GeV² (circles, dashed) and $W = 82$ GeV, $Q^2 = 8$ GeV² (squares, solid). The integrated cross section with $t_{\text{cut}} = -1$ GeV² versus Q^2 for $W = 82$ [89] GeV (middle) and versus W for $Q^2 = 8$ [9.6] GeV² (right) are compared with H1 (circles, dashed) [ZEUS (squares, solid)] data [2]. The statistical and systematic errors are added in quadrature.

relation $F_2 = 2x_{\text{Bj}}F_1$, valid to LO accuracy, leads to the known double log approximation in DIS:

$$F_2(x_{\text{Bj}}, Q^2) \approx \frac{4x_{\text{Bj}}}{3\pi} \Im m \mathcal{H}^{\text{DL}}(2x_{\text{Bj}}, t = 0, 2Q^2) \quad (10)$$

(the factor two in scale dependence is explained by [11]).

The interpretation of Eq. (9) is depicted in Fig. 1(c), where the evolution operator, i.e., the (k_{\perp} ordered) re-summation of the gluonic ladder, is inserted in the hand-bag diagram. Only the moment with $n = 1$ is needed as non-perturbative input. It might be interpreted as a non-local gluon operator with dimension three and spin one that is sandwiched between the proton states. Since in the light-cone gauge this operator formally reduces to a local operator, we might argue that its matrix element is ξ independent. In accordance with quark counting rules, predicting the power fall at large $|t|$, a simple multipole ansatz with unknown slope B_G is used:

$$G_1(\eta, t, Q_0^2) \equiv G_1(t) = \frac{N_G}{(1 - B_G t/3)^3}. \quad (11)$$

The DVCS process is accessible via the photon lepto-production and interferes with the Bethe-Heitler Bremsstrahlung one. For small x_{Bj} the DVCS cross section dominates, the interference is negligible (after integration over the azimuthal angle), and the Bethe-Heitler cross section, known in terms of the elastic proton form factors, can be subtracted [2]. Theoretically, the DVCS cross section for small x_{Bj} is safely approximated by [10]

$$\frac{d\sigma_T}{dt}(W, t, Q^2) \approx \frac{4\pi\alpha^2}{Q^4} |\xi \mathcal{H}^S(\xi, t, Q^2)|^2 \Big|_{\xi = \frac{Q^2}{2W^2 + Q^2}}. \quad (12)$$

A fit of the cross section, using Eqs. (8)–(12), to H1 and ZEUS data [2] provide the parameter set

$$N_G = 1.97, \quad B_G = 3.68 \text{ GeV}^{-2}, \quad Q_0^2 = 0.51 \text{ GeV}^2, \quad (13)$$

where $n_f = 3$ and $\Lambda_{\text{QCD}} = 150$ MeV were fixed. Note that the t -slope is rather robust under a change of Λ_{QCD} , however, it is sensitive to the form factor shape. For an exponential ansatz it decreases to $B_G^{\text{exp}} = 2.58 \text{ GeV}^{-2}$.

Let us confront these findings with DIS data in the kinematic region that is considered here. Within the parameters (13) the double log approximation (10) reasonably describes the shape of data. However, the normalization can fail of up to 30%. Radiative QCD corrections are important [16] and it is stated that the normalization discrepancy in DVCS is resolved at next-to-leading order [17]. A closer look to this problem, beyond next-to-leading order, will be presented somewhere else [18].

The dominance of the pomeron allows us now to reveal the singlet quark and gluonic GPDs, which are represented by a Mellin-Barnes integral [12, 13]. In the double log approximation they read, e.g., for vanishing skewness, as

$$xH^G(x, \eta=0) \simeq I_0(\sigma, \bar{\alpha}t) \left[\frac{\alpha_s(Q)}{\alpha_s(Q_0)} \right]^{\bar{\lambda}^+} G_1(t) + \dots, \quad (14)$$

$$xH^{\Sigma}(x, \eta=0) \simeq \frac{n_f}{9} \rho I_1(\sigma, \bar{\alpha}t) \left[\frac{\alpha_s(Q)}{\alpha_s(Q_0)} \right]^{\bar{\lambda}^+} G_1(t) + \dots,$$

where $\sigma(\xi = 2x)$ and $\bar{\alpha}(\xi = 2x)$ is set, see below Eq. (8). They reduce for $t = 0$ to the common parton densities.

For $\eta = 0$ the Fourier transform of H with respect to the transverse momentum transfer $\Delta_{\perp} = (\mathbf{P}_2 - \mathbf{P}_1)_{\perp}$,

$$\rho = \iint \frac{d^2\Delta_{\perp}}{(2\pi)^2} e^{i\mathbf{b}\cdot\Delta_{\perp}} H(x, \eta = 0, t = -\Delta_{\perp}^2, Q^2), \quad (15)$$

has a probabilistic interpretation [19]. In the infinite momentum frame the proton is viewed as a disc with a mean square charge radius $r^2 = 4 \frac{\partial}{\partial t} F_1(t) \Big|_{t=0} \approx (0.6 \text{ fm})^2$. The density of partons is given by $\rho(x, \mathbf{b}, Q^2)$, depending on momentum fraction x , transverse distance \mathbf{b} from the proton center, and resolution $1/Q$. The mean square distance for a parton species is proportional to the t -slope

$$\langle \mathbf{b}^2 \rangle = 4B, \quad B = \frac{\partial}{\partial t} \ln H(x, \eta = 0, t, Q^2) \Big|_{t=0}. \quad (16)$$

In Fig. 3(a) the averaged distance $\langle \mathbf{b}^2 \rangle^{1/2}$ is displayed for both gluons and sea quarks. Compared to the charge

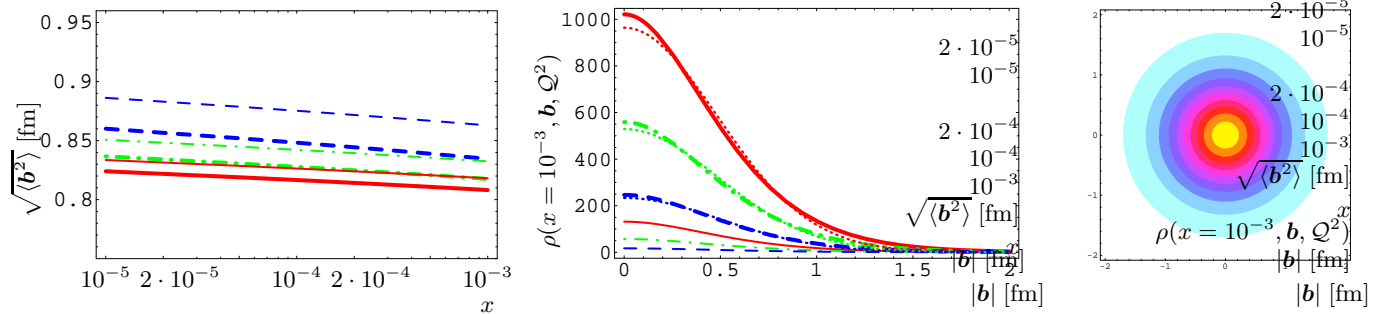


FIG. 3: The root of the mean square distance (16) for gluons (thick) and singlet quarks (thin) and the corresponding parton densities (15) versus $|b|$ are shown in the left and middle panel, respectively, for $x = 10^{-3}$. Q^2 is set to 2 GeV^2 (dashed), 10 GeV^2 (dash-dotted), and 100 GeV^2 (solid). The dotted lines in the middle panel display the result for an exponential t -dependence. In the right panel the transverse distribution of gluons is visualized, where $x = 10^{-3}$ and $Q^2 = 10 \text{ GeV}^2$.

radius $r \simeq 0.6 \text{ fm}$, this distance is of about 40–50% larger. Within an exponential form factor ansatz this inflation would shrink to 20–30%. The weakly grow with decreasing x and fall with increasing Q arise from the intertwining of soft-pomeron input and evolution. The double log asymptotics, i.e., (8), (14), and (16), shed light on this:

$$B(W, Q^2) \simeq B_G + \frac{\alpha'_p \ln^{\frac{1}{2}}(4W^2/Q^2)}{\sqrt{\lambda} \ln^{\frac{1}{2}}(\alpha_s(Q_0)/\alpha_s(Q))}. \quad (17)$$

Such a behavior was also experimentally observed in hard vector meson electroproduction, dominated by the gluon exchange. Moreover, the measured t -slope of the cross section is consistent with our findings for DVCS [20]. In Fig. 3(b) it can be realized that the sea quark density is a bit broader and as known from forward parton densities much smaller than the gluon one. The gluon density within the exponential form factor ansatz is displayed by dotted lines. For $|b| \lesssim 1.5 \text{ fm}$ the density only slightly differs from that of the multipol ansatz. A further characteristic is that the densities (start to) vanish for $|b| \gtrsim 1.5 \text{ fm}$, see panel (c). However, the multipol ansatz induces a long tail that results into an enlargement, compared to the exponential one, of the averaged distance.

In this letter we argued that the soft pomeron trajectory essentially determines the gluonic GPD at a small resolution scale and that perturbative evolution can be used to arrive at higher scales, where factorization holds true. This interplay of non-perturbative and perturbative QCD leads to a realistic behavior of the DVCS amplitude. To illuminate this, the double log approximation has been derived and used to LO. It was checked that a numerical treatment, with changed normalization and scale parameter, essentially leads to the same results. The fit to experimental data provides the non-perturbative parameter and reveals so the 3D gluon and sea quark distributions inside the proton. The theoretical framework can be refined and confronting it with precise DVCS data would strongly constrain the non-perturbative ansatz.

This project has been supported by the U.S. National Science Foundation under grant no. PHY-0456520.

-
- [1] D. Müller, D. Robaschik, B. Geyer, F.-M. Dittes and J. Horejši, *Fortschr. Phys.* **42**, 101 (1994); X. Ji, *Phys. Rev. Lett.* **78**, 610 (1997); A. Radyushkin, *Phys. Lett.* **B380**, 417 (1996).
 - [2] C. Adloff *et al.* (H1 Coll.), *Phys. Lett.* **B517**, 47 (2001); ZEUS, S. Chekanov *et al.*, *Phys. Lett.* **B573**, 46 (2003); H1, A. Aktas *et al.*, *Eur. Phys. J.* **C44**, 1 (2005).
 - [3] A. Donnachie and P. V. Landshoff, *Nucl. Phys.* **B244**, 322 (1984); *ibid.* **B267**, 690 (1986).
 - [4] A. Donnachie and P. V. Landshoff, *Phys. Lett.* **B437**, 408 (1998); *ibid.* **B518**, 63 (2001).
 - [5] I. I. Balitsky and L. N. Lipatov, *Sov. J. Nucl. Phys.* **28**, 822 (1978); E. A. Kuraev, L. N. Lipatov and V. S. Fadin, *Sov. Phys. JETP* **45** 199 (1977).
 - [6] M. Glück, E. Reya and A. Vogt, *Z. Phys.* **C48**, 471 (1990); *Eur. Phys. J.* **C5**, 461 (1998).
 - [7] R. D. Ball and S. Forte, *Phys. Lett.* **B336**, 77 (1994).
 - [8] A. V. Kotikov and G. Parente, *Nucl. Phys.* **B549**, 242 (1999).
 - [9] H1, S. Aid *et al.*, *Z. Phys.* **C69**, 27 (1995); ZEUS, S. Chekanov *et al.*, *Nucl. Phys.* **B627**, 3 (2002).
 - [10] A. V. Belitsky, D. Müller and A. Kirchner, *Nucl. Phys.* **B629**, 323 (2002).
 - [11] Note that we define $Q^2 = -(q_1 + q_2)^2/4$, which coincides with $Q^2 = -q_1^2$ only in the forward case.
 - [12] D. Müller and A. Schäfer, *Nucl. Phys.* **B739**, 1 (2006).
 - [13] M. Kirch, A. Manashov and A. Schäfer, *Phys. Rev. Lett.* **95**, 012002 (2005); *Phys. Rev.* **D72**, 114006 (2005).
 - [14] G. Ingelman and P. E. Schlein, *Phys. Lett.* **B152**, 256 (1985).
 - [15] ZEUS, M. Derrick *et al.*, *Phys. Lett.* **B356**, 129 (1995).
 - [16] A. V. Belitsky, D. Müller, L. Niedermeier and A. Schäfer, *Phys. Lett.* **B474**, 163 (2000).
 - [17] A. Freund, M. McDermott and M. Strikman, *Phys. Rev.* **D67**, 036001 (2003).
 - [18] D. Müller, *Phys. Lett.* **B634**, 227 (2006); K. Kumerički, D. Müller, K. Passek-Kumerički and A. Schäfer, in preparation.
 - [19] M. Burkardt, *Phys. Rev.* **D62**, 071503 (2000); *Int. J. Mod. Phys.* **A18**, 173 (2003); A. V. Belitsky, D. Müller, *Nucl. Phys. A* **711**, 118 (2002).
 - [20] C. Adloff *et al.* (H1 Coll.), *Eur. Phys. J.* **C13**, 371 (2000).